

Effects of Empirical Versus Model-Based Reflectance Calibration on Automated Analysis of Imaging Spectrometer Data: A Case Study from the Drum Mountains, Utah

John L. Dwyer, Fred A. Kruse, and Adam B. Lefkoff

Abstract

Data collected by the Airborne Visible/Infrared Imaging Spectrometer (AVIRIS) have been calibrated to surface reflectance using an empirical method and an atmospheric model-based method. Single spectra extracted from both calibrated data sets for locations with known mineralogy compared favorably with laboratory and field spectral measurements of samples from the same locations. Generally, spectral features were somewhat subdued in data calibrated using the model-based method when compared with those calibrated using the empirical method. Automated feature extraction and expert system analysis techniques have been successfully applied to both data sets to produce similar endmember probability images and spectral endmember libraries. Linear spectral unmixing procedures applied to both calibrated data sets produced similar image maps. These comparisons demonstrated the utility of the model-based approach for atmospherically correcting imaging spectrometer data prior to extraction of scientific information. The results indicated that imaging spectrometer data can be calibrated and analyzed without a priori knowledge of the remote target.

Introduction

The increasing availability of imaging spectrometer data provides Earth scientists with a new source of information to conduct quantitative studies of Earth-surface materials, particularly the spatial variability of their physical and chemical properties (Goetz *et al.*, 1985). The Airborne Visible/Infrared Imaging Spectrometer (AVIRIS) was flown on an ER-2 aircraft at an altitude of 25 km and acquires 224 contiguous spectral bands of data in the 0.4- to 2.45- μm wavelength region of the electromagnetic spectrum (Porter and Enmark, 1987). Each band corresponds to a nominal wavelength interval of 9.7 nm, and the spatial resolution of each pixel was approxi-

mately 17m by 17m. A typical AVIRIS "data cube" is dimensioned as 512 lines by 614 samples and 224 bands.

Quantitative determination of the physical and chemical characteristics of Earth-surface materials requires conversion of AVIRIS data to physical units so that analytical results can be compared and validated with field and laboratory measurements. The objective of this study was to evaluate the scientific utility of two different techniques for calibrating AVIRIS data to ground reflectance, an empirically based method and a model-based method. If the model-based calibrated data could be used successfully with automated mapping techniques to produce maps showing the spatial distribution of surface mineralogy, then future operational mapping could be conducted using AVIRIS data without a priori knowledge.

The AVIRIS data of the Drum Mountains, Utah, were collected on 26 September 1989. Those data were calibrated using the empirical line method (Roberts *et al.*, 1985; Conel *et al.*, 1987; Kruse *et al.*, 1990a) and an atmospheric-model-based technique (Gao and Goetz, 1990; CSES, 1992). Spectra of surface materials were extracted from each of the calibrated data sets and were compared to laboratory spectra of pure mineral samples and field reflectance spectra of rocks and soils measured in the study area. Spectra also were extracted from the same pixels in each of the calibrated AVIRIS data sets to assess differences between the resultant spectral reflectance curves. The different calibration methods were evaluated with respect to the performance of automated feature extraction techniques coupled with expert system decision rules to identify the predominant mineral constituents of each pixel. The study also examined the effect of the model-based calibration on the results of the linear spectral unmixing technique (Boardman, 1991) used to derive mineral abundance estimates on a pixel-by-pixel basis.

Drum Mountains Study Area

The Drum Mountains area, located in the semiarid terrain of west-central Utah (Figure 1), was selected as the field site because of the good exposure of diverse rock types and alteration mineralogy. The geology of the area is well docu-

J.L. Dwyer is with Hughes STX Corporation, EROS Data Center, Sioux Falls, SD 57198.

F.A. Kruse was with the Center for the Study of Earth from Space, Cooperative Institute for Research in Environmental Sciences, University of Colorado-Boulder, Boulder, CO 80309 and is currently with Analytical Imaging and Geophysics LLC, Louisville, CO 80027.

A.B. Lefkoff is with BSC Limited Liability Company, Boulder, CO 80309.

Photogrammetric Engineering & Remote Sensing,
Vol. 61, No. 10, October 1995, pp. 1247-1254.

0099-1112/95/6110-1247\$3.00/0
© 1995 American Society for Photogrammetry
and Remote Sensing

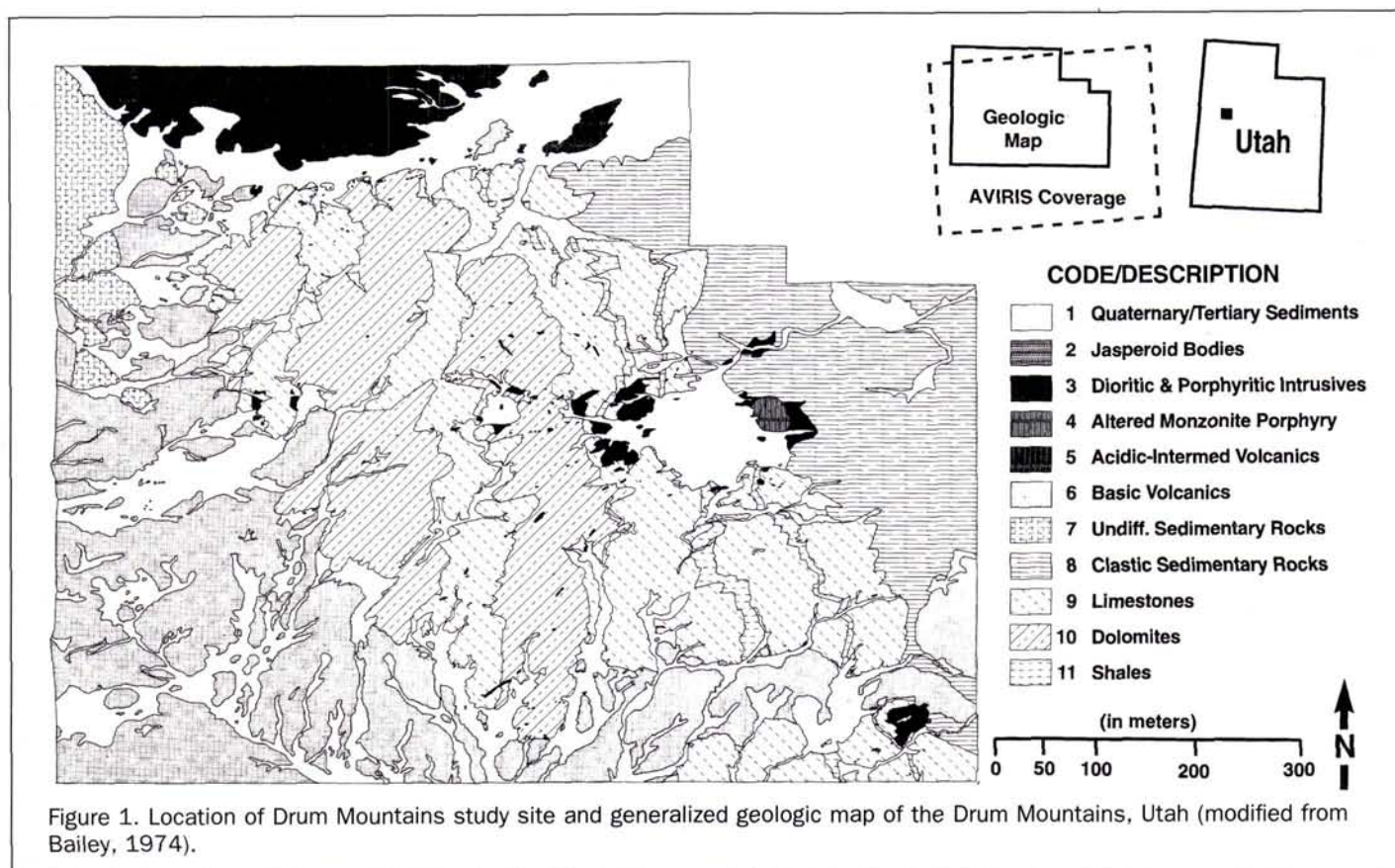


Figure 1. Location of Drum Mountains study site and generalized geologic map of the Drum Mountains, Utah (modified from Bailey, 1974).

mented (Bailey, 1974; Lindsay, 1979), and a variety of other remotely sensed and ground-based data have been acquired to support evaluation of the AVIRIS data.

Rocks exposed in the study area include a thick sequence of west-dipping Cambrian limestones, dolomites, and shales, which overlie a thicker, heterogeneous sequence of Cambrian and Precambrian quartzite and argillite. Intermediate to felsic Tertiary volcanic rocks occur in fault contact with sedimentary rocks in the northern part of the study area, and older intermediate to mafic Tertiary volcanic rocks overlie the same sedimentary units on the west and south. The volcanic rocks have been hydrothermally altered in places, and some carbonate rocks adjacent to the volcanics have been bleached and recrystallized.

A contact metamorphic aureole characterized by the development of calcsilicate mineralization in limestone and shale units occurs in the central part of the study area. The aureole is associated with two small stocks. One of the intrusives is a diorite (code 3 in Figure 1) and is unaltered where exposed. The other was probably a monzonite (code 4 in Figure 1), but it has undergone such intense hydrothermal alteration that the original lithology is uncertain (Bailey, 1974).

AVIRIS Calibration

There has been a significant amount of published work documenting the spectral reflectance characteristics of minerals (Hunt and Salisbury, 1970; Clark *et al.*, 1990; Kruse and Hauff, 1992) as a function of transitions in the electronic and vibrational energy states of atoms and bonds, respectively, that define the structure of minerals. These physical and

chemical properties allow identification of mineral species on the basis of diagnostic absorption features contained in the reflectance spectra (Goetz, 1981). Quantitative analysis and interpretation of AVIRIS spectra require conversion of measurement units from at-sensor radiance values ($\mu\text{W cm}^{-2} \text{nm}^{-1} \text{sr}^{-1}$) to percent reflectance.

Two calibration methods were applied to the Drum Mountains AVIRIS data. One approach, referred to as an empirical line calibration method (ELREF) (Roberts *et al.*, 1985; Conel *et al.*, 1987; Kruse *et al.*, 1990a), involves the use of laboratory or field spectral reflectance measurements for spectrally and spatially homogeneous bright and dark calibration targets that can be easily located in the imagery. Pixels corresponding to the calibration sites were extracted from the AVIRIS data and were used to compute an average radiance spectrum for each target. A linear regression model of the average radiance spectra and the corresponding field reflectance spectra was used to derive coefficients that, in turn, were used to linearly transform the AVIRIS radiance values to ground reflectance. The coefficients were applied to all pixels for each band in the image. The general form of the equation was

$$R_{\lambda} = G_{\lambda}L_{\lambda} + O_{\lambda} (+ \epsilon_{\lambda})$$

where R_{λ} the calculated reflectance for band λ , G_{λ} is the gain for channel λ , L_{λ} is the at-sensor radiance for band λ , O_{λ} is the offset for band λ , and ϵ_{λ} is the error term from the regression for band λ . This method is constrained by the need for prior acquisition of spectral reflectance measurements for the calibration targets.

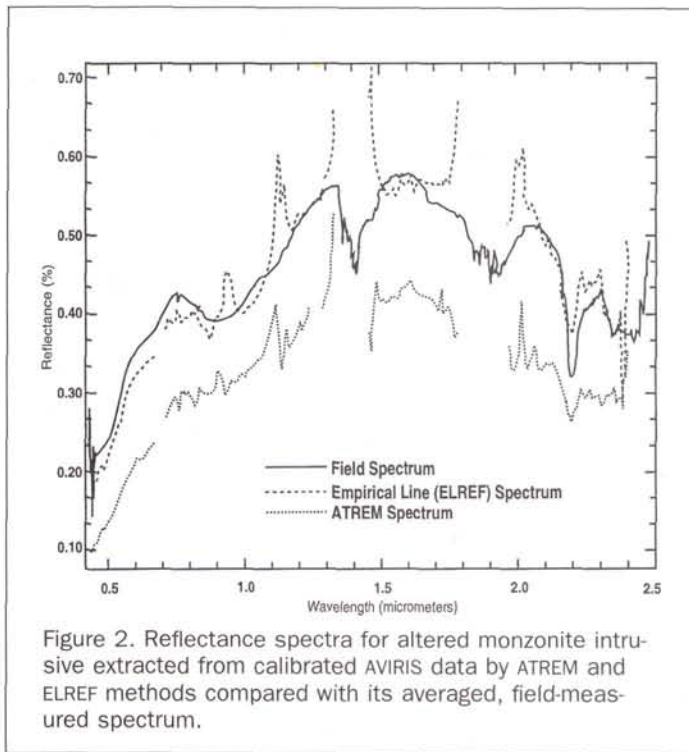


Figure 2. Reflectance spectra for altered monzonite intrusive extracted from calibrated AVIRIS data by ATREM and ELREF methods compared with its averaged, field-measured spectrum.

The other calibration method applied to the Drum Mountains AVIRIS data was based on a radiative transfer model-based technique (ATREM) (Gao and Goetz, 1990; CSES, 1992) which calculates water vapor on a pixel-by-pixel basis

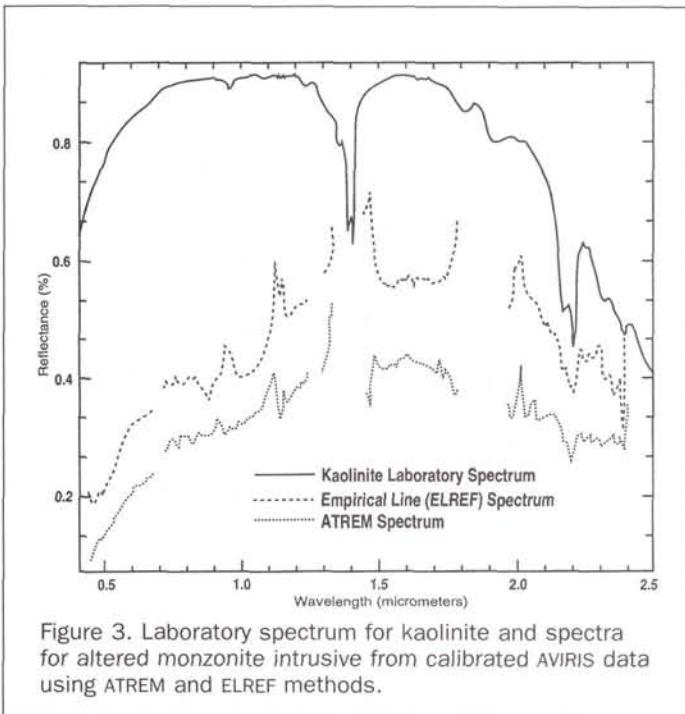


Figure 3. Laboratory spectrum for kaolinite and spectra for altered monzonite intrusive from calibrated AVIRIS data using ATREM and ELREF methods.

TABLE 1. SUMMARY OF RESULTS FROM LABORATORY ANALYSES OF ROCK SAMPLES FOR ALTERED MONZONITE INTRUSIVE (GEOLOGIC UNIT TMP) (FROM TREMPER, 1991)

Sample Tmp-1

Description of hand specimen: Fresh surfaces are generally gray and white phenocrysts (clay). Weathered surfaces are many shades of brown.

Thin section examination: The rock appears altered in thin section and contains 70% quartz, 25% clay, and 5% hematite.

X-ray diffraction: Whole-quartz, kaolinite
Major-kaolinite, quartz
Minor-
Trace-

Sample Tmp-6

Description of hand specimen: This is altered Tmp. The "freshest" surfaces are white and contain altered (clay) phenocrysts and brown deposits. Weathered surfaces are dominated by shades of brown.

Thin section examination: NA

X-ray diffraction: Whole-quartz, illite/muscovite
Major-quartz, illite/muscovite
Minor-
Trace-montmorillonite

using the 0.94- and 1.10- μ m water vapor absorption bands. The solar zenith angle was calculated on the basis of latitude and longitude of the AVIRIS scene center, and the date and time of data acquisition. Apparent reflectance spectra were obtained by dividing each AVIRIS radiance spectrum by spectrally equivalent values for solar irradiance above the atmosphere (Kneizys *et al.*, 1988). A number of theoretical water vapor transmittance spectra for the 0.94- and 1.10- μ m water vapor bands were calculated for varying amounts of water vapor using an approximate radiative transfer code (5S) (Tanre *et al.*, 1986) and the Malkmus (1967) narrow band spectral model. The modeled spectra were subjected to a three-band ratioing procedure to generate a look-up table of water vapor concentrations that was, in turn, used to convert the AVIRIS "apparent reflectance" measurements to total water vapor in the atmospheric column. This procedure, the ATREM method (CSES, 1992), was used to generate an image that shows the spatial distribution of various water vapor concentrations derived for each pixel in the AVIRIS image. The water vapor image was used, along with the transmittance spectra derived for atmospheric gases (CO_2 , O_3 , N_2O , CO , CH_4 , and O_2) using the Malkmus narrow band model and the 5S code, to produce scaled surface reflectance (Teillet, 1989; Gao and Goetz, 1990; CSES, 1992). Thus, without *a priori* knowledge, this model-based technique produced an image depicting estimates of total atmospheric water vapor and an AVIRIS data set calibrated to surface reflectance.

Evaluation of Calibration Results

Spectra were extracted from each of the calibrated data sets to qualitatively compare results of the two methods, as well as for comparison with field spectra measured at the study site contemporaneous with the AVIRIS overflight. Sample sites were selected on the basis of coincident field spectroradiometer measurements and petrographic, X-ray diffraction (XRD), and geochemical analyses (Temper, 1991) performed on samples that could be referenced to AVIRIS pixels. Figure 2 shows reflectance spectra extracted from each of the cali-

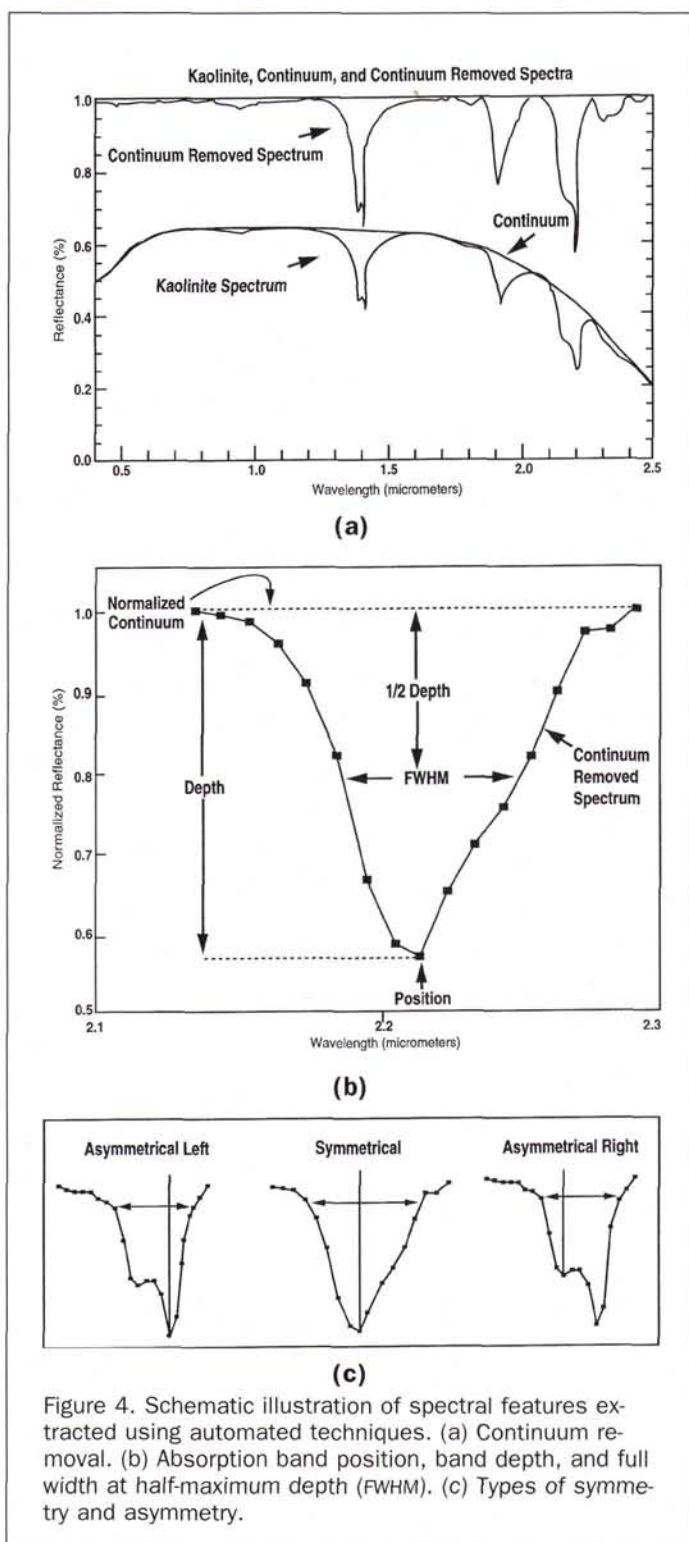


Figure 4. Schematic illustration of spectral features extracted using automated techniques. (a) Continuum removal. (b) Absorption band position, band depth, and full width at half-maximum depth (FWHM). (c) Types of symmetry and asymmetry.

shape of the major absorption features for Fe³⁺ (near 0.9 μm) and for clays (near 2.2 μm). AVIRIS spectra were compared to a laboratory measurement for kaolinite in Figure 3, which demonstrates that the presence of kaolinite (based on the asymmetrical absorption feature near 2.2 μm) can be resolved in both field and AVIRIS data. Table 1 summarizes results from laboratory and petrographic studies performed on samples from the same location.

Automated Feature Extraction and Expert System Analysis

Although an experienced scientist can determine mineralogy through interpretation of reflectance spectra, the large volume of spectral information in an AVIRIS data set renders manual analysis of individual pixel spectra time prohibitive. A computerized expert system or knowledge-based approach to spectral feature extraction was developed to overcome this limitation and to exploit the information content of AVIRIS data (Kruse *et al.*, 1990b; Kruse *et al.*, 1993). In this system, automated procedures that emulate the cognitive processes of an experienced analyst were developed to extract and characterize absorption features in reflectance spectra. A "table of facts" is automatically compiled, against which knowledge-based decision rules can be applied to identify minerals and assign probabilities for matching the target spectrum with an entry in a spectral library. The process involves computing and removing a continuum for reference spectra (Figure 4a), and then characterizing each spectral absorption feature in terms of (1) the wavelength position of the absorption band minimum, (2) its absorption band depth, (3) its full width at half maximum band depth (Figure 4b), and (4) the asymmetry of its shape (Figure 4c).

These four characteristics were computed for selected library spectra to create a fact table such as is shown in Table 2. Facts become "rules" when modified according to an analyst's knowledge and experience. Operationally, the set of decision rules is constructed and applied to generate a specific set of outputs (Table 3).

The two calibrated AVIRIS data sets were analyzed using the expert system procedures. The ATREM and ELREF calibrated image cubes were processed using continuum removal and spectral feature characterization techniques, and end-member probability images were generated that show similar absorption features and mineralogy for both data sets. The

TABLE 2. EXAMPLE OF FACTS TABLE USED IN FORMULATING EXPERT SYSTEM DECISION RULES

Position	Depth	Full Width at Half Maximum Depth (μm)	Asymmetry
2.20500	0.43205	0.07103	-0.36491
2.16500	0.28542	0.08045	0.45323
1.41300	0.34993	0.04437	-0.16448
1.39300	0.31137	0.04938	0.24484
1.53400	0.01815	0.30250	-1.23977
1.55200	0.01356	0.31923	-1.33787
1.56400	0.01315	0.32115	-1.40374
1.91500	0.24424	0.05789	0.29967
2.31500	0.07358	0.08988	0.51287
2.35500	0.06062	0.09350	-0.24663
2.37500	0.05160	0.09602	-0.68974
0.94900	0.02389	0.05829	0.20893
0.97000	0.02369	0.05864	-0.10375
0.98200	0.01521	0.12519	-0.22758
1.01800	0.01417	0.12685	-0.57116

TABLE 3. EXAMPLE OF DECISION RULES USED BY EXPERT SYSTEM TO IDENTIFY MINERALS

Example: kaolinite vs. alunite.

1st decision (rock level)

if spectra has a deep band in 2.15 to 2.22 μm region
then look for similar spectra in "clay" species.

2nd decision ("clay" species)

if it has a doublet near 2.2 μm
and strongest band of the doublet is 2.21 μm
and weakest band of the doublet is near 2.17 μm
and 2.21 μm asymmetry is $\ll 1$ (left asymmetry)
and 2.17 μm asymmetry is $\gg 1$ (right asymmetry)
and additional smaller bands near 2.32, 2.36, and 2.38 μm
then it is **kaolinite**.

if it has a broad band near 2.17 μm
and a weak shoulder near 2.21 μm
and 2.17 μm asymmetry is $\ll 1$ (Left asymmetry)
and additional weaker bands are near 2.32 and 2.42 μm
then it is **alunite**.

endmember probability images, each of which is a best estimate image showing the spectrally dominant mineral for a given pixel, were used to develop an endmember library for each calibrated data set. The library consisted of average spectra for the best endmembers identified using the expert system (Figure 5).

Spectral Linear Unmixing

The spectral signature for each pixel is the combined spectral response of all included surface materials (vegetation, rock, soil, shadow, etc.). Assuming that each material's contribution to the combined response is directly related to its exposed areal extent within the pixel, the spectrum from an AVIRIS pixel can be modeled as a linear combination of individual endmember spectra (Adams *et al.*, 1986; Mustard and Pieters, 1987). A spectral linear unmixing model can be formulated (Boardman, 1990; Boardman, 1991) to estimate the fractional abundance of each endmember that best accounts for the observed mixed spectrum of an AVIRIS pixel. A suite of mineral endmember spectra (Figure 5), determined using the automated procedures described above, were extracted from each of the calibrated AVIRIS data sets and used as inputs to a spectral unmixing model. The spatial distribution of fractional abundance estimates for the mineral endmembers unmixed using the ELREF and ATREM calibrated data sets are generally similar (Plate 1).

Maps derived from spectral linear unmixing compare favorably with the geologic map for the study area (Figure 1). Such a comparison must take into account the fact that the geological map represents lithologies based on age, assemblage, texture, and other physical characteristics, while the AVIRIS-based maps represent the response of mineral content alone (and for only the top 50 μm of its exposed surface). An indication supporting the potential utility of AVIRIS data for geologic mapping is the fact that the spatial distribution of dolomite mapped using the AVIRIS data generally conforms to that shown on the geologic map. In addition, the distribution of clay minerals mapped using the AVIRIS data is limited to units known to contain those specific clay minerals based on X-ray diffraction and petrographic results. Although these initial results were generally satisfactory, further work is required to validate the results in detail, particularly to deter-

mine the mineralogical composition of the "other" endmember using field measurements and laboratory analyses of samples.

One notable difference between the unmixing results for the two methods is the difference between their respective maps of the distribution of illite. The image produced using the empirical line method shows the illite distribution to be spatially contiguous and distinctly different from the other endmembers, whereas the ATREM method shows substantial overlap with the halloysite area. This is indicative of two problems encountered in using the ATREM calibrated data. First, the ATREM method tends to reduce the size of mineral

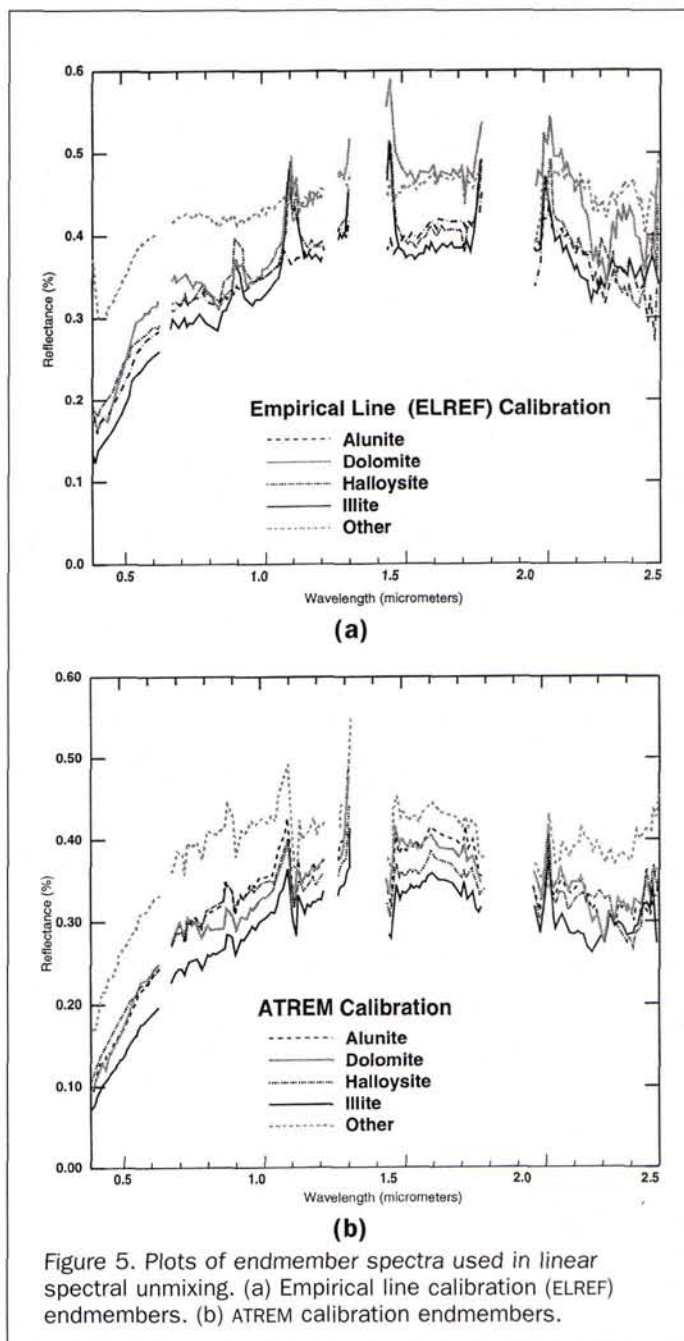
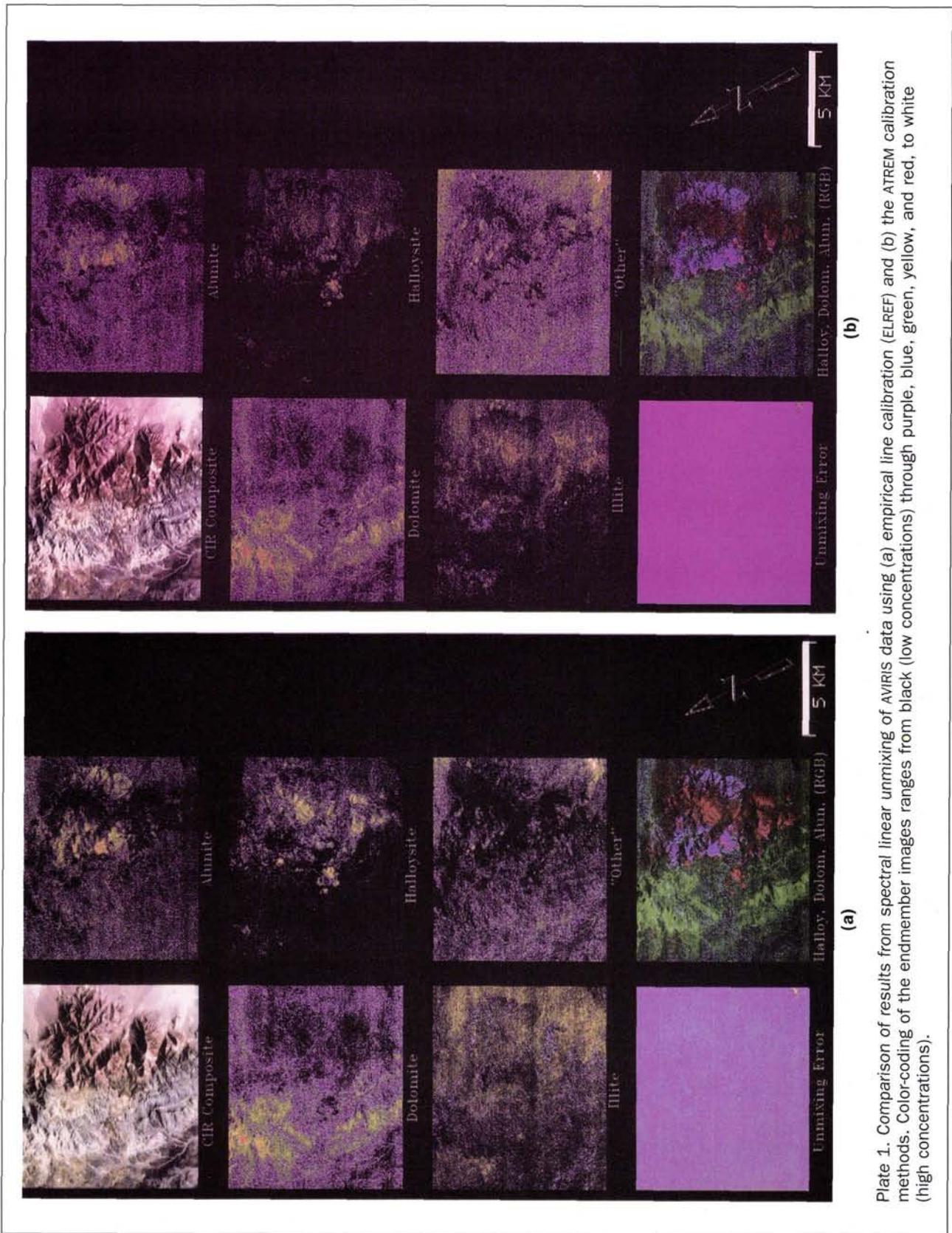


Figure 5. Plots of endmember spectra used in linear spectral unmixing. (a) Empirical line calibration (ELREF) endmembers. (b) ATREM calibration endmembers.



absorption features as compared to the empirical line method. The ATREM data were actually closer to absolute reflectance and more representative of the field conditions. However, for feature-based analysis techniques, deeper absorption features such as those resulting from ELREF calibration are easier to find and analyze. By comparing the illite versus halloysite endmember spectra for both calibration techniques (Figure 5), it was clear that the two endmembers are more similar in the ATREM data than in the empirical line data. Secondly, the ATREM method appears to be more sensitive to noise in the data. The feature-based technique used to extract the endmembers generally is not very noise tolerant and, consequently, better results are obtained for data calibrated with the empirical line method. In this study, the signal-to-noise ratio of the AVIRIS data presented the greatest obstacle to automated analysis of spectral absorption features.

Conclusions

The empirical line (ELREF) and ATREM calibration methods each produce spectra similar to laboratory and field measurements of representative samples from the same pixel locations. The empirical line method appears to enhance absorption feature band depth, a characteristic that has been observed in results from other data sets. This enhancement allows automated spectral feature extraction techniques and expert system analyses to perform better on data calibrated using this approach. In the ATREM calibrated data, mineral absorption features are somewhat subdued. In addition, we observed that the ATREM model overcorrects for water absorption bands in the 0.9 μm wavelength region and, consequently, inhibits detection of shallow absorption features associated with the iron-oxide minerals.

The results from the expert system analysis and spectral unmixing are generally similar using the two calibration methods, although unmixing results can vary by as much as 30 percent when similar endmembers are used for the ATREM calibration (i.e., illite endmember). The disparity observed here is presumed to be related to the spectral similarity of the illite and halloysite endmembers in the ATREM calibrated data, which causes a degeneracy of the spectral library. Based on these results, the model-based approach is considered a viable alternative technique for atmospheric correction of imaging spectrometer data that can be used without *a priori* information (e.g., field measurements). When compared with the empirical line technique, which requires ground measurements as a prerequisite to calibration, the model-based approach offers a major advantage for operational imaging spectrometer data investigations. From this study, it is apparent that calibration procedures can have a significant affect on scientific investigations. Extraction of quantitative results from imaging spectrometer data, such as those derived from linear spectral unmixing, must be performed with a clear understanding of the assumptions inherent to the calibration models that are applied.

Acknowledgments

This research was funded by the U. S. Geological Survey under cooperative agreement 14-08-0001-A0746. J.L. Dwyer's work was performed under U.S. Geological contract 1434-92-C-40004.

References

- Adams, J.B., M.O. Smith, and P.E. Johnson, 1986. Spectral mixture modeling: A new analysis of rock and soil types at Viking Lander 1, *Journal of Geophysical Research*, 91:8113-8125.
- Bailey, G. Bryan, 1974. *The Occurrence, Origin, and Economic Significance of Gold-Bearing Jasperoids in the Central Drum Mountains, Utah*, Ph.D. Dissertation, Stanford University, 300 p.
- Boardman, J.W., 1990. Inversion of high spectral resolution data, *Proceedings, Society of Photo-Optical Instrumentation Engineers (SPIE)*, 1298:222-233.
- , 1991. *Sedimentary Facies Analysis Using Imaging Spectrometry: A Geophysical Inverse Problem*, Ph.D. dissertation, University of Colorado, 212 p.
- Center for the Study of Earth from Space (CSES), 1992. *ATMospheric REMoval Program (ATREM), Version 1.1*, University of Colorado, Boulder, Colorado, 24 p.
- Clark, R.N., T.V.V. King, M. Klejwa, and G.A. Swayze, 1990. High spectral resolution reflectance spectroscopy of minerals, *Journal of Geophysical Research*, 95(B8):12,653-12,680.
- Conel, J.E., R.O. Green, G. Vane, C.J. Bruegge, and R.E. Alley, 1987. Airborne Imaging Spectrometer-2: Radiometry and a comparison of methods for the recovery of ground reflectance, *Proceedings, Airborne Imaging Spectrometer Data Analysis Workshop*, Jet Propulsion Laboratory 87-30, Pasadena, California, pp.18-47.
- Gao, B., and F.H. Goetz, 1990. Column atmospheric water vapor and vegetation liquid water retrievals from airborne imaging spectrometer data, *Journal of Geophysical Research*, 95(D4):3549-3564.
- Goetz, F.H.A., 1981. Spectroscopic remote sensing for geologic applications, *Proceedings, Society of Photo-Optical Instrumentation Engineers (SPIE)*, 268:17-21.
- Goetz, A.F.H., Greg Vane, J.E. Solomon, and B.N. Rock, 1985. Imaging spectrometry for earth remote sensing, *Science*, 228:1147-1153.
- Hunt, G.R., and J.W. Salisbury, 1970. Visible and near-infrared reflectance spectra of minerals and rocks, I. Silicate Minerals, *Modern Geology*, 1:219-228.
- Kneizys, F.X., E.P. Shettle, L.W. Abreau, J.H. Chetwynd, G.P. Anderson, W.O. Gallery, E.A. Selby, and S.A. Clough, 1988. *Users Guide to LOWTRAN 7*, AFGL-TR-8-0177, Air Force Geophysics Laboratory, Bedford, Massachusetts, 137 p.
- Kruse, F.A., K.S. Kierein-Young, and J.W. Boardman, 1990a. Mineral mapping at Cuprite, Nevada, with a 63 channel imaging spectrometer, *Photogrammetric Engineering & Remote Sensing*, 56(1): 83-92.
- Kruse, F.A., O. Seznec, and P.M. Krotkov, 1990b. An expert system for geologic mapping with imaging spectrometers, *Proceedings, Application of Artificial Intelligence VIII*, Society of Photo-Optical Instrumentation Engineers (SPIE), 1293:904-917.
- Kruse, F.A., and P.L. Hauff (editors), 1992. *The IGCP-264 Spectral Properties Database*, AGU Special Publication, 211 p. (in press).
- Kruse, F.A., A.B. Lefkoff, and J.B. Dietz, 1993. Expert system-based mineral mapping in northern Death Valley, California/Nevada using the Airborne Visible/Infrared Imaging Spectrometer (AVIRIS), *Remote Sensing of Environment*, 44(2/3):309-336.
- Lindsey, D.L., 1979. *Geologic Map and Cross-Sections of Tertiary Rocks in the Thomas Range and Northern Drum Mountains, Juab County, Utah*, U.S. Geological Survey Miscellaneous Investigation Series Map I-1176, Washington, D.C., scale 1:62,500.
- Malkmus, W., 1967. Random Lorentz band model with exponential-tailed S line intensity distribution function, *J. Opt. Soc. Am.*, 57: 323-329.
- Mustard, J.F., and C.M. Pieters, 1987. Quantitative abundance estimates from bidirection reflectance measurements, *Proceedings, Lunar Planet Science Conference, 17th, Part 2, Journal of Geophysical Research*, supplement, 92(B4):E617-E626.
- Porter, W.M., and H.T. Enmark, 1987. A system overview of the Airborne Visible/Infrared Imaging Spectrometer (AVIRIS), *Proceedings, Society of Photo-Optical Instrumentation Engineers (SPIE)*, 834:22-31.
- Roberts, D.A., Y. Yamaguchi, and R.J.P. Lyon, 1985. Calibration of airborne imaging spectrometer data to percent reflectance using field spectral measurements, *Proceedings, Nineteenth Interna-*

tional Symposium on Remote Sensing of Environment, Ann Arbor, Michigan, 21-25 October, pp. 679-688.

Tanre, D., C. Deroo, P. Duhaut, M. Herman, J.J. Morcrette, J. Perbos, and P.Y. Deschamps, 1986. *Simulation of the Satellite Signal in the Solar Spectrum (5S) Users Guide*, Laboratoire d'Optique Atmospherique, U.S.T. de Lille, 59655 Villeneuve d'Ascq, France.

Teillet, P.M., 1989. Surface reflectance retrieval using atmospheric correction algorithms. *Proceedings of IGARSS'89 and the 12th Canadian Symposium on Remote Sensing*, Vancouver, Canada, pp. 864-867.

Tremper, C.W., 1991. *The Mineralogy and Chemistry of Rocks from the Drum Mountains, West-Central Utah*, unpublished internal report to the U.S. Geological Survey (P.O. #2451234), Department of Geology, Northern Illinois University, DeKalb, Illinois, 76 p.

(Received 6 January 1994; accepted 9 May 1994; revised 3 August 1994)



John L. Dwyer

John L. Dwyer received his B.S. degree in Geology from St. Lawrence University and an M.Sc. degree in Geological Sciences from the University of Colorado-Boulder. Mr. Dwyer has over 17 years experience in remote sensing and geographic information systems applications in such areas as environmental planning, energy and mineral resource assessment, and glacial geology. Mr. Dwyer is currently the Hughes STX Corporation Project Staff Scientist at the EROS Data Center in Sioux Falls, South Dakota. His research interests include integrated spatial data analysis for mineral resource assessment, the development and application of digital image analysis techniques for environmental monitoring and studies of landscape change, and the analysis of multisensor data sets for geoscience investigations.

Fred A. Kruse
Dr. Fred A. Kruse received the B.S. degree in geology from the University of Massachusetts, Amherst, in 1976. He earned both the M.S. (1984) and Ph.D. degrees (1987) in geology from the Colorado School of Mines, Golden, Colorado.

Dr. Kruse served as a Topographic Engineer Officer in the United States Army Corps of Engineers (1976 to 1981) and with the Remote Sensing Section of the U.S. Geological Survey, Branch of Geophysics (1982-1987). He is presently Deputy Director, Center for the Study of Earth from Space (CSES); Fellow, Cooperative Institute for Research in Environmental Sciences (CIRES); and Assistant Research Professor, Department of Geological Sciences, all within the University of Colorado, Boulder. Dr. Kruse's primary research interests are in the application of remote sensing technology to the areas of ore deposits, their regional occurrence and distribution, and geologic evolution. Other research activities include development of visualization techniques for interactive image analysis and use of artificial intelligence (AI) techniques for identifying and mapping Earth-surface materials. As a member of NASA's Shuttle Imaging Radar-C (SIR-C) team, Dr. Kruse is combining imaging spectrometer and radar analysis results to address geologic problems relating to geomorphic development of the land surface.

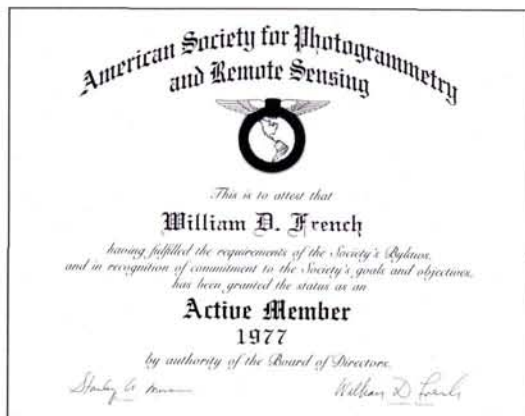
Adam B. Lefkoff

Mr. Adam B. Lefkoff is a 1990 graduate of the University of California, San Diego, with a B.A. in Computer Science (Cum Laude). While at UCSD, he was the recipient of an Education Abroad Scholarship, which allowed him to spend a year at Flinders University of South Australia (1989-90). Presently, Mr. Lefkoff is an independent consultant and author of a commercial software system for interactive analysis and visualization of multispectral remote sensing data and other raster images. At the time this paper was written, Mr. Lefkoff was a Senior Applications Programmer (1990-93) at the Center for the Study of Earth from Space (CSES), Cooperative Institute for Research in Environmental Sciences (CIRES), University of Colorado, Boulder, Colorado. He was the lead programmer for development of the Spectral Image Processing System (SIPS) and the Radar Analysis and Visualization Environment (RAVEN), two showcase interactive image processing systems written in the Interactive Data Language (IDL).

ASPRS MEMBERSHIP CERTIFICATES

See your name in Print!
Purchase your beautiful newly designed ASPRS Membership Certificate.

Active and Student Member Certificates are available for only \$10. Certificates can be order individually or payment can be added to your Membership Dues.



Size: 11" x 14"
ASPRS Logo is Metallic Blue with a Gold overlay.

To order your certificate contact:
ASPRS Membership
at 301-493-0290;
fax: 301-493-0208;
email: members@asprs.org.